Available online at www.eccomasproceedia.org
Eccomas Proceedia COMPDYN (2023) 1983-1995

ECCOMAS
Proceedia

COMPDYN 2023
9th ECCOMAS Thematic Conference on
Computational Methods in Structural Dynamics and Earthquake Engineering
M. Papadrakakis, M. Fragiadakis (eds.)
Athens, Greece, 12-14 June 2023

PERSITALTIC DRIVEN FLOWS IN PIEZOELECTRIC POROUS DYNAMIC METAMATERIALS - HOMOGENIZATION BASED MODELLING

E. Rohan[1], **and V. Lukeš**[1]

[1] Department of Mechanics, NTIS New Technologies for Information Society, Faculty of Applied Sciences, University of West Bohemia, Univerzitní 8, 306 00 Pilsen, Czech Republic
e-mail: rohan@kme.zcu.cz, vlukes@kme.zcu.cz

Abstract. *The paper deals with the homogenization-based modelling of periodic porous structures saturated by a Newtonian fluid and locally controlable due to embedded piezoelectric segments which can induce a peristaltic deformation of the microchannels, in response to prescribed propagating voltage waves. The two-scale homogenized problem is nonlinear by the consequence deformation-dependent homogenized coefficients in the macroscopic equations. For this, a linear expansions based on the sensitivity analysis of the homogenized coefficients with respect to the deformation induced by the macroscopic quantities is employed. A special care is needed to apply this approach to the dynamic permeability which is involved in the time convolution integrals. This approximate treatment of the non-linearity is justified as far as the deformations are moderate. As an advatage, it enables to reduce the computational cost not exceeding much the one of linear problems. At the same time, the nonlinearity is important to capture the pumping effect of the porous material in a case of time periodic actuation by electric field.*

Keywords: Peristaltic deformation, Fluid flow, Homogenization, Porous media, Piezoelectric actuation

ISSN:2623-3347
Peer-review under responsibility of the organizing committee of COMPDYN 2023.
doi: 10.7712/120123.10536.21328

1 INTRODUCTION

Fluid flow in porous materials can be generated by the peristaltic deformation of pores in time; this important principle is well known in physiology, biology, and tissue biomechanics, [5, 1, 8, 4], however, as a driving mechanism of fluid transport, it presents and important and challenging issue in the design of smart "bio-inspired" materials.

The desired peristaltic deformation wave propagating in the porous material can be induced by various phenomena. In electroactive materials, such a deformation wave can be produced by locally controlled electric field [10]. Alternatively, actuating electric wave can be coupled with acoustic waves [11], whereby the actuators can compensate damping associated with the transported fluid viscosity.

To explore functionality of such metamaterial structures, we develop computational tools based on the multiscale homogenization approach. The computational models arise from the homogenization of the dynamic fluid-structure interaction problem, taking into account nonlinear effects.

We derived a homogenized model of a piezo-poroelastic material which enables to transport fluid against small pressure slope. As the new contribution, all the inertia effects in the deforming skeleton and in the flowing fluid are considered. This feature presents a nontrivial extension of the quasistatic model in the context of the deformation-dependent homogenized coefficients.

To capture the peristaltic effects, nonlinear phenomena related to deformation are considered in an approximate way to keep the computational modelling effective as much as possible. For this, a linearization procedure is applied, being based on the sensitivity analysis of the local characteristic responses with respect to the macroscopic strains and pressures which modify the deformed configurations of the representative volume elements at the micro-level [9]. In this way, by virtue of the methodology introduced in [9], we get first-order expansions of all the homogenized coefficients; also the sensitivity of the dynamic permeability constituting the convolution kernel is treated. The peristaltic flow in the porous structure is described by a nonlinear Darcy law with hydraulic permeability reflecting the deformed configuration of the local microstructure. The numerical results illustrate some specific properties of the considered active porous structures, namely the controlable transport of the fluid according to the propagating acoustic and electric field waves.

We consider locally periodic porous structures occupying domain $\Omega_s^\varepsilon \subset \Omega \subset \mathbb{R}^3$, saturated by a Newtonian fluid flowing in channels $\Omega_f^\varepsilon = \Omega \setminus \overline{\Omega_s^\varepsilon}$, whereby ε is the microstructure scale. Besides an elastic-dielectric part Ω_e^ε, the solid phase $\Omega_s^\varepsilon = \Omega_e^\varepsilon \cup \Omega_z^\varepsilon \cup \Omega_*^\varepsilon$ contains piezoelectric segments $\Omega_z^\varepsilon \subset \Omega_s^\varepsilon$ which can induce peristaltic deformation wave of the microchannels in response to the locally controlled electric field due to distributed electrodes $\Omega_*^\varepsilon \subset \Omega_s^\varepsilon$ connected to an external circuit. Such a structure presents a smart material, transforming a propagating electric potential wave into a peristaltic deformation wave propelling the fluid.

This paper presents some important issues to cope with when extending the homogenization problem for the dynamic flow, namely respecting the inertia in the fluid. First we introduce the micromodel which is subject of the asymptotic homogenization using the unfolding method [3], whereby a relevant scaling by ε of some micromodel parameters must be introduced. Then two different situations of respecting the flow dynamics are discussed.

2 MICROMODEL AND THE FLUID-STRUCTURE INTERACTION PROBLEM

In the piezoelectric solid, the Cauchy stress tensor $\boldsymbol{\sigma}^\varepsilon$ and the electric displacement $\vec{D}^\varepsilon$ depend on the strain tensor $\boldsymbol{e}(\boldsymbol{u}^\varepsilon) = (\nabla \boldsymbol{u}^\varepsilon + (\nabla \boldsymbol{u}^\varepsilon)^T)/2$ defined in terms of the displacement field

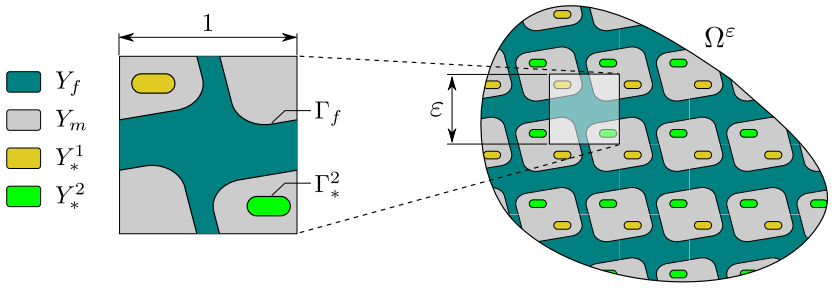

Figure 1: Periodic microstructures and the representative cell Y decomposition.

$\boldsymbol{u}^\varepsilon = (u_i^\varepsilon)$, and on the electric field $\vec{E}(\varphi^\varepsilon) = \nabla\varphi^\varepsilon$ defined in terms of the electric potential φ^ε. The following constitutive equations characterize the piezoelectric solid in Ω_s^ε and, thereby, for vanishing $\underline{\boldsymbol{g}}^\varepsilon$, also the elastic parts in Ω_e^ε and Ω_*^ε (infinite $\boldsymbol{d}^\varepsilon$),

$$\sigma_{ij}^\varepsilon(\boldsymbol{u}^\varepsilon,\varphi^\varepsilon) = A_{ijkl}^\varepsilon e_{kl}^\varepsilon(\boldsymbol{u}^\varepsilon) - g_{kij}^\varepsilon E_k^\varepsilon(\varphi^\varepsilon)\ , \quad D_k^\varepsilon(\boldsymbol{u}^\varepsilon,\varphi^\varepsilon) = g_{kij}^\varepsilon e_{ij}^\varepsilon(\boldsymbol{u}^\varepsilon) + d_{kl}^\varepsilon E_l^\varepsilon(\varphi^\varepsilon)\ , \tag{1}$$

where $\mathbb{A}^\varepsilon = (A_{ijkl}^\varepsilon)$ is the elasticity symmetric positive definite tensor satisfying $A_{ijkl} = A_{klij} = A_{jilk}$, the deformation is coupled with the electric field through the 3rd order tensor $\underline{\boldsymbol{g}}^\varepsilon = (g_{kij}^\varepsilon)$, $g_{kij}^\varepsilon = g_{kji}^\varepsilon$ and $\boldsymbol{d} = (d_{kl})$ is the electric permittivity tensor. We consider a Newtonian barotropic fluid characterized by the dynamic viscosity μ^ε, a reference density ρ_f and the fluid compressibility γ, such that the stress tensor is

$$\boldsymbol{\sigma}_f^\varepsilon = -p^\varepsilon \boldsymbol{I} + 2\mu^\varepsilon(\mathbb{I} - \frac{1}{3}\boldsymbol{I}\otimes\boldsymbol{I})\boldsymbol{e}(\boldsymbol{v}^{f,\varepsilon})\ . \tag{2}$$

The micromodel involves the following differential equations governing the fluid-solid interaction and the electric field coupled with the deformation through the piezoelectric constitutive law (1),

$$\begin{aligned}
\rho_s\ddot{\boldsymbol{u}}^\varepsilon - \nabla\cdot\boldsymbol{\sigma}_s^\varepsilon(\boldsymbol{u}^\varepsilon,\varphi^\varepsilon) &= \boldsymbol{f}^{s,\varepsilon}\ , \quad \text{in } \Omega_{m*}^\varepsilon\ ,\\
-\nabla\cdot\vec{D}^\varepsilon(\boldsymbol{u}^\varepsilon,\varphi^\varepsilon) &= 0\ , \quad \text{in } \Omega_m^\varepsilon\ ,\\
\rho_f\left(\dot{\boldsymbol{v}}^{f,\varepsilon} + (\boldsymbol{w}^\varepsilon\cdot\nabla)\boldsymbol{v}^{f,\varepsilon}\right) + \nabla p^\varepsilon - \mu^\varepsilon\nabla^2\boldsymbol{v}^{f,\varepsilon} &= \boldsymbol{f}^{f,\varepsilon}\ ,\\
\gamma\dot{p} + \nabla\cdot\boldsymbol{v}^{f,\varepsilon} &= 0\ , \quad \text{in } \Omega_f^\varepsilon\ ,
\end{aligned} \tag{3}$$

where $\boldsymbol{f}^{d,\varepsilon}, d = s, f$ are the body forces. Note that the "dot" means the material derivative and the seepage velocity $\boldsymbol{w}^\varepsilon = \boldsymbol{v}^{f,\varepsilon} - \dot{\tilde{\boldsymbol{u}}}^\varepsilon$ is defined using an extension $\dot{\tilde{\boldsymbol{u}}}^\varepsilon$ of the solid phase velocity.

The homogenization procedure based on the periodic unfolding method [3] is applied to the weak formulation of (3) which yields the following equations to be satisfied by admissible

solutions $(\boldsymbol{u}^\varepsilon(t,\cdot),\varphi^\varepsilon(t,\cdot),\boldsymbol{w}(t,\cdot),\bar{p}^\varepsilon(t,\cdot)) \in \mathbf{S}^\varepsilon(\Omega)$

$$
\begin{aligned}
&\int_{\Omega^\varepsilon_{m*}} \left(\mathbb{A}^\varepsilon \boldsymbol{e}(\boldsymbol{u}^\varepsilon) - \underline{\boldsymbol{g}}^\varepsilon \nabla\varphi^\varepsilon\right) : \boldsymbol{e}(\boldsymbol{v}^\varepsilon) \\
&\qquad - \int_{\Gamma^\varepsilon_{fs}} \boldsymbol{n}^\varepsilon \otimes \boldsymbol{v}^\varepsilon : \boldsymbol{\sigma}^\varepsilon_f(\boldsymbol{w}^\varepsilon, \dot{\tilde{\boldsymbol{u}}}, p^\varepsilon) = \int_{\Omega^\varepsilon_{m*}} \boldsymbol{f}^{s,\varepsilon}\cdot\boldsymbol{v}^\varepsilon + \int_{\partial_\sigma\Omega^\varepsilon_{m*}} \boldsymbol{b}^{s,\varepsilon}\cdot\boldsymbol{v}^\varepsilon \,, \\
&\int_{\Omega^\varepsilon_m} \left((\underline{\boldsymbol{g}}^\varepsilon)^T : \boldsymbol{e}(\boldsymbol{u}^\varepsilon) + \boldsymbol{d}^\varepsilon\nabla\varphi^\varepsilon\right)\cdot\nabla\psi^\varepsilon = \int_{\Omega^\varepsilon_m} \rho^\varepsilon_E\psi^\varepsilon \,, \\
&\int_{\Omega^\varepsilon_f} \left(2\mu^\varepsilon \boldsymbol{e}(\boldsymbol{w}^\varepsilon + \dot{\tilde{\boldsymbol{u}}}^\varepsilon) - p^\varepsilon \boldsymbol{I}\right) : \boldsymbol{e}(\boldsymbol{\theta}^\varepsilon) = \int_{\Omega^\varepsilon_f} \boldsymbol{f}^{f,\varepsilon}\cdot\boldsymbol{\theta}^\varepsilon \,, \\
&\int_{\Omega^\varepsilon_f} q^\varepsilon \left(\gamma\dot{p}^\varepsilon + \nabla\cdot(\boldsymbol{w}^\varepsilon + \dot{\tilde{\boldsymbol{u}}})\right) = 0 \,,
\end{aligned}
\tag{4}
$$

for all admissible test fuctions $(\boldsymbol{v}^\varepsilon,\psi^\varepsilon,\boldsymbol{\theta}^\varepsilon,q^\varepsilon) \in \mathbf{S}^\varepsilon_0(\Omega)$. Here we need not specify the admissibility sets $\mathbf{S}^\varepsilon(\Omega)$ and $\mathbf{S}^\varepsilon_0(\Omega)$ which must respect all the Dirichlet type boundary conditions; note that the seepage velocity $\boldsymbol{w}^\varepsilon$ and the pressure are defined in the pores only, whereby $\boldsymbol{w}^\varepsilon = 0$ on the pore walls Γ^ε_{fs}.

2.1 Periodic microsctructure and the representative cell decomposition

The periodic microstructure is generated by a rescaled reference periodic cell $Y =]0,1[^3$ decomposed into non-overlapping subdomains Y_m, Y_f and Y_*, see Fig. 1, $Y = Y_m \cup Y_f \cup Y_*$, such that $Y_m = Y_e \cup Y_z$, where the subdomains Y_d generate corresponding domains Ω^ε_d, $d = e, z, *, f$. For the device functionality, at least two groups of separated electrodes $\Omega^{\alpha,\varepsilon}_*$, $\alpha = 1, 2$ represented by $Y^\alpha_* \subset Y_*$ must be considered.

The union of all the interfaces, Γ_Y, splits in two disjoint parts (in the sense of the surface measure), assuming $\partial Y_f \cap \partial Y_* = \emptyset$ (the conductors separated from the fluid)

$$
\begin{aligned}
&\Gamma_Y = \Gamma_{fs} \cup \Gamma_{m*} \,, \quad \Gamma_{fs} = \overline{Y_s} \cap \overline{Y_f} \,, \\
&\Gamma^\alpha_{m*} = \overline{Y^\alpha_*} \cap \overline{Y_m} \,, \quad \Gamma_{m*} = \bigcup_\alpha \Gamma^\alpha_{m*} \,.
\end{aligned}
\tag{5}
$$

We also assume well separated conductor parts, *i.e.* $\overline{Y^\alpha_*} \cap \partial Y = \emptyset$, such that the periodic lattice Ω^α_* is constituted by mutually disconnected inclusions with the perimeter $\approx \varepsilon$.

2.2 Scaling of the material parameters

To retain specific features of the micromodel (3) in the homogenization limit $\varepsilon \to 0$, some of the involved material parameters are considered to depend on ε. To allow for microstructures with strongly controlled electric field, in formulation (3), spatially constant potentials $\bar{\varphi}^\alpha$ are given for each simply connected domain $\Omega^{\alpha,\varepsilon}_*$ occupied by the perfect conductor and represented by Y^α_* within the cell Y. The following assumptions are made:

$$
\begin{aligned}
&\text{a) Strongly controlled field:} \quad \varphi^\varepsilon = \bar{\varphi}^\alpha \text{ in } \Omega^{\alpha,\varepsilon}_* \,, \\
&\text{b) Weakly piezoelectric material:} \ \underline{\boldsymbol{g}}^\varepsilon(x) = \varepsilon\underline{\bar{\boldsymbol{g}}} \,, \quad \boldsymbol{d}^\varepsilon(x) = \varepsilon^2\bar{\boldsymbol{d}} \,, \quad \text{in } \Omega^\varepsilon_m \,, \\
&\text{c) viscous flow with the nonslip condition on pore walls,} \quad \mu^\varepsilon = \varepsilon^\beta\bar{\mu} \,, \quad \text{in } \Omega^\varepsilon_f \,,
\end{aligned}
\tag{6}
$$

where $\beta = 2$, or $\beta = 3/2$, depending on the flow dynamics approximation. Above, the scaling b) is the consequence of the locally controlled electric field, a).

3 HOMOGENIZATION AND THE MACROSCOPIC MODEL

Neglecting the advection term $(\boldsymbol{w}^\varepsilon \cdot \nabla)\boldsymbol{v}^{f,\varepsilon}$ in (3) leads to the same scaling, as in the quasi-static case, $\beta = 2$ in (6)(c). By th econsequence, the following truncated expansions (the so-called recovery sequences) of displacements, electric potential, pressure and the fluid seepage velocity are applied to derive the limit equations,

$$\begin{aligned}
\mathcal{T}_\varepsilon(\boldsymbol{u}^\varepsilon) &\approx \boldsymbol{u}^{R\varepsilon}(x,y) := \boldsymbol{u}^{0\varepsilon}(x) + \varepsilon \boldsymbol{u}^{1\varepsilon}(x,y)\ ,\\
\mathcal{T}_\varepsilon(\varphi^\varepsilon) &\approx \varphi^{R\varepsilon}(x,y) := \hat\varphi^{0\varepsilon}(x,y)\ ,\\
\mathcal{T}_\varepsilon(p^\varepsilon) &\approx p^{R\varepsilon}(x,y) := p^{0\varepsilon}(x) + \varepsilon p^{1\varepsilon}(x,y)\ ,\\
\mathcal{T}_\varepsilon(\widetilde{\boldsymbol{w}}^\varepsilon) &\approx \widetilde{\boldsymbol{w}}^{R\varepsilon}(x,y) := \hat{\boldsymbol{w}}(x,y)\ ,
\end{aligned} \tag{7}$$

where all the two-scale functions depending on $x \in \Omega$, $y \in Y$ (and also on time t – this is not indicated in the notation) are Y-periodic in y.

The homogenization using the approach explained in [11] provides an extension of the piezo-poroelastic model derived in [10] for disconnected porosity. The macroscopic displacement $\boldsymbol{u}^0$, the flow seepage $\boldsymbol{w}^0$ and pressure p^0 satisfy the following coupled equations involving the homogenized (effective) coefficients $\mathbb{H} := (\mathbb{A}, \boldsymbol{B}, M, Z^\alpha, \boldsymbol{H}^\alpha)$ of the piezo-poroelastic model, and the dynamic permeability $\boldsymbol{K}(t)$, such that

$$\begin{aligned}
\bar\rho \partial^2_{tt}\boldsymbol{u}^0 + \phi_f\rho_f\partial_t\boldsymbol{w} - \nabla\cdot\left(\mathbb{A}\boldsymbol{e}(\boldsymbol{u}) - p^0\boldsymbol{B} + \sum_\alpha \boldsymbol{H}^\alpha\bar\varphi^\alpha\right) &= \hat{\boldsymbol{f}}\ ,\\
\boldsymbol{B}:\boldsymbol{e}(\partial_t\boldsymbol{u}^0) + M\partial_t p^0 + \nabla\cdot\boldsymbol{w} &= \sum_\alpha Z^\alpha\partial_t\bar\varphi^\alpha\ ,
\end{aligned} \tag{8}$$

$$\text{where}\quad \boldsymbol{w}(t,x) = -\frac{1}{\bar\mu}\int_0^t \boldsymbol{K}(t-s)(\nabla p(s,\cdot) + \rho_f\partial_{tt}\boldsymbol{u}^0 - \boldsymbol{f}^f(s,\cdot))\,\mathrm{d}t\ ,$$

where $\bar\rho$ and $\phi_f\rho_f$ are the effective densities of the mixture and of the fluid, respectively. For a suitable given electric potential control $\{\bar\varphi^\alpha\}_\alpha(t,x)$, a peristaltic deformation wave propagates. However, model (8) can induce a fluid flow opposed to the one caused by the pressure gradient only when the nonlinearity associated with respecting the deformed configuration effect of the homogenized coefficients is captured. For this, we suggest and approximate treatment using the sensitivity analysis enabling to replace homogenized coefficients represented by $\mathbb{H}$ using $\tilde{\mathbb{H}}$ given by the linear formulae obtained using the sensitivity analysis approach, as exlained briefly in Section 4.

3.1 Local limit flow equations, the dynamic Darcy law

We consider the model with neglected advection inertia in the flow for which the dynamic permeability $\widehat{\mathcal{K}}_{ij}$ is obtained using characteristic responses $w_i^j(y,t)$ of the non-steady Stokes flow, see [11], where the acoustic problem in steadily perfused porous media was treated. Further we employ the space of Y-periodic functions, namely

$$\begin{aligned}
\mathbf{H}^1_{\#0}(Y_f) &= \{\boldsymbol{v} \in \widetilde{\mathbf{H}}^1_\#(Y_f)|\ \boldsymbol{v} = \boldsymbol{0} \text{ on } \Gamma_{fs}\}\ ,\\
H^1_{\#0*}(Y_m) &= \{\psi \in H^1_\#(Y_m)|\ \psi = 0 \text{ on } \Gamma_*\}\ .
\end{aligned} \tag{9}$$

For a. a. $x \in \Omega$, the limit $\varepsilon \to 0$ of the non-steady Stokes flow yields the local problem: Find $(\hat{\boldsymbol{w}}(t,x,\cdot), p^1 t, x, \cdot)) \in \mathbf{H}^1_{\#0}(Y_f) \times H^1_{\#0*}(Y_m)$, such that

$$\begin{aligned} &\rho_f \fint_{Y_f} \partial_t \hat{\boldsymbol{w}} \cdot \hat{\boldsymbol{\theta}} + \fint_{Y_f} \bar{\mu} \nabla_y \hat{\boldsymbol{w}} : \nabla_y \hat{\boldsymbol{\theta}} + \fint_{Y_f} \nabla_y p^1 \cdot \hat{\boldsymbol{\theta}} = (\widehat{\boldsymbol{f}}^f - \nabla_x p^0 - \rho_f \partial_{tt} \boldsymbol{u}^0) \cdot \fint_{Y_f} \hat{\boldsymbol{\theta}} \ , \\ &\fint_{Y_f} q^1 \nabla_y \cdot \hat{\boldsymbol{w}} = 0 \ , \end{aligned} \tag{10}$$

for all $(\hat{\boldsymbol{\theta}}, q^1) \in \mathbf{H}^1_{\#0}(Y_f) \times H^1_{\#0*}(Y_m)$. We shall employ the following substitution,

$$\boldsymbol{p}^{dyn} := (\nabla_x p^0 + \rho_f \ddot{\boldsymbol{u}}^0 - \widehat{\boldsymbol{f}}^f)/\rho_f \ . \tag{11}$$

Using the Laplace transformation applied in (10) and the decomposition $\hat{\underset{\sim}{\boldsymbol{w}}} = \underset{\sim}{\boldsymbol{w}}^j \underset{\sim}{p}{}^{dyn}_j$, the dynamic permeability can be introduced (in the time domain) by virtue of the characteristic response $\boldsymbol{w}^j = (w_i^j)$,

$$\begin{aligned} \boldsymbol{w}(t,x) &= -\int_0^t \boldsymbol{\mathcal{K}}(t,s) \frac{\mathrm{d}}{\mathrm{d}\, s} \boldsymbol{p}^{dyn}(s,x)\, \mathrm{d}s - \boldsymbol{\mathcal{K}}(t,0) \boldsymbol{p}^{dyn}(0,x) \ , \\ \text{with} \quad \mathcal{K}_{ij} &= -\fint_{Y_f} w_i^j \ , \end{aligned} \tag{12}$$

The characteristic response $\boldsymbol{w}^j = (w_i^j)$ is the solution of (10) with the substitution (11), computed for loading by the unit volume dynamic force $\boldsymbol{p}^{dyn} := \mathbf{e}^j = (\delta_{1,j}, \delta_{2,j}, \delta_{3,j})$ in the respective direction.

3.2 Two-scale limit of the equilibrium and fluid mass conservation

The limit two-scale mass conservation is obtaiend from $(3)_4$ using the ansatz (7), which yields

$$\gamma \phi_f \partial_t p^0 + \nabla_x \cdot \boldsymbol{w} + \phi_f \nabla_x \cdot \boldsymbol{u}^0 - \fint_{Y_s} \nabla_y \cdot \boldsymbol{u}^1 = 0 \quad \text{a.e. in } \Omega \ , \tag{13}$$

where $\boldsymbol{w}(t,x) = \phi_f \boldsymbol{w}^0(t,x)$ is expressed in terms of the dynamic Darcy law (12).

The two-scale limit equilibrium of the solid skeleton interacting with fluid flow can be derived in analogy with [11] concerning the the treatment of the interaction term $\tilde{\mathcal{I}}^\varepsilon(\tilde{\boldsymbol{\sigma}}_f^\varepsilon, \boldsymbol{v}^\varepsilon)$, as described below. To get rid of the stress gradient on the interface Γ_{fs}, namely involving $\bar{\mu} \nabla_y^2 \hat{\boldsymbol{w}}$, the local flow equation integrated in Y_f is employed; from (10), upon integrating by parts, we get

$$\fint_{Y_f} \bar{\mu} \nabla_y^2 \hat{\boldsymbol{w}} - \fint_{Y_f} \nabla_y p^1 = \fint_{Y_f} \rho_f \partial_t \hat{\boldsymbol{w}} - (\widehat{\boldsymbol{f}}^f - \nabla_x p^0 - \rho_f \partial_{tt}^2 \boldsymbol{u}^0) \phi_f \ , \tag{14}$$

since all other terms vanish due to the local incompressibility of velocities and the Y-periodicity of all two-scale functions. Thus, using (14), we get

$$\begin{aligned} &\tilde{\mathcal{I}}^\varepsilon(\tilde{\boldsymbol{\sigma}}_f^\varepsilon, \boldsymbol{v}^\varepsilon) = \int_{\Gamma_{fs}^\varepsilon} \boldsymbol{n}^s \cdot \boldsymbol{\sigma}_f^\varepsilon \cdot \boldsymbol{v}^\varepsilon \to \\ &\to \int_\Omega \phi_f \left(p^0 \nabla + \widehat{\boldsymbol{f}}^f - \rho_f (\ddot{\boldsymbol{u}}^0 + \dot{\boldsymbol{w}}^0) \right) \cdot \boldsymbol{v}^0 - \int_\Omega p^0 \fint_{\Gamma_{fs}} \boldsymbol{v}^1 \cdot \boldsymbol{n}^s + \int_{\partial_\sigma \Omega} \phi_f \widehat{\boldsymbol{b}}^f \cdot \boldsymbol{v}^0 \ . \end{aligned}$$

Then the limit equilibrium equation associated with the solid skeleton attains the following form,

$$\int_\Omega \bar\rho_s \ddot{\boldsymbol{u}}^0\cdot\boldsymbol{v}^0 + \int_\Omega \fint_{Y_s} \mathbb{A}(\boldsymbol{e}_x(\boldsymbol{u}^0)+\boldsymbol{e}_y(\boldsymbol{u}^1)) : (\boldsymbol{e}_x(\boldsymbol{v}^0)+\boldsymbol{e}_y(\boldsymbol{v}^1))$$
$$- \fint_{\Omega\times Y_m} \boldsymbol{e}_y(\boldsymbol{v}^1) : \underline{\bar{\boldsymbol{g}}}^T\nabla_y\hat\varphi^0 - \int_\Omega \phi_f\left(p^0\nabla\cdot - \rho_f(\ddot{\boldsymbol{u}}^0+\ddot{\boldsymbol{w}}^0)\right)\cdot\boldsymbol{v}^0 + \int_\Omega p^0 \fint_{\Gamma_{fs}} \boldsymbol{v}^1\cdot\boldsymbol{n}^s \qquad (15)$$
$$= \int_\Omega \widetilde{\boldsymbol{f}}\cdot\boldsymbol{v}^0 + \int_{\partial_\sigma\Omega}\widetilde{\boldsymbol{b}}\cdot\boldsymbol{v}^0\ ,$$

for all admissible test functions, $\boldsymbol{v}^0\in\mathbf{S}_0(\Omega)$ and $\boldsymbol{v}^1\in\mathbf{H}^1_\#(Y_s)$, where $\bar\rho_s$ is the mean density in Y_s and $\widetilde{\boldsymbol{f}},\widetilde{\boldsymbol{b}}$ denote the effective loads.

4 Approximation of deformation-dependent homogenized coefficients

Using the asymptotic analysis w.r.t. the scale $\varepsilon\to 0$, pursuing our previous work [10], we have developed a nonlinear homogenized model of such a smart porous material which describes the peristaltic-driven flow under a quasistatic regime, so disregarding any inertia effects [12]. Although the deformations are small and the channels do not collapse (the channel lumen is not closing completely by the deformation), the homogenized model can mimic the peristalsis-driven flow provided nonlinearity arising due to deformed configuration is accounted for conveniently. For this, we employed an approximation which leads to a nonlinear model as the consequence of the effective model parameters (tensors) depending on the solution by virtue of the homogenization respecting locally deforming microstructures [9].

Using the sensitivity analysis approach explained in [9], all the coefficients $\mathbb{H}$ in (8) can be replaced by $\tilde{\mathbb{H}}$ introduced using the first order expansion formulae which have the generic form

$$\tilde{\mathbb{H}}(\boldsymbol{e}(\boldsymbol{u}),p) = \mathbb{H}^0 + \delta_{\boldsymbol{e}}\mathbb{H}^0 : \boldsymbol{e}(\boldsymbol{u}) + \delta_p\mathbb{H}^0 p + \sum_\alpha \delta_{\varphi,\alpha}\mathbb{H}^0\bar\varphi^\alpha\ , \qquad (16)$$

where $\delta_\spadesuit\mathbb{H}^0$ is the gradient w.r.t. the macroscopic quantity $\spadesuit$. In the case of the permeability $\boldsymbol{K}(t)$, an expansion analogous to (16) based on the sensitivity analysis is not obvious. A possible treatment is based on the spectral decomposition of the seepage $\boldsymbol{w}$ using the eigenfunctions $\{\boldsymbol{\omega}^r\}_r$ and eigenvalues $\{\lambda^r\}_r$ of an eigenvalue problem associated with the Stokes flow problem in Y_f

Then the seepage is expressed using the basis $\{\boldsymbol{\omega}^r\}_r$, so that $\boldsymbol{w}(t,x,y)=\sum_r\boldsymbol{\omega}^r(y)\vartheta^r(t,x)$. Respecting the deformation of the microconfiguration due to the response at time t makes the eigenpairs $(\boldsymbol{\omega}^r_{(t)},\lambda^r_{(t)})$ to depend on t, as indicated by $_{(t)}$. Upon denoting by $\langle v\rangle_{Y_f}=|Y|^{-1}\int_{Y_f}v$ the average, the seepage is given by

$$\boldsymbol{w}(t,x) = -\int_0^t \boldsymbol{\mathcal{K}}(t,s)\boldsymbol{p}^{dyn}(s,x)\,\mathrm{d}s = \sum_r \left\langle\boldsymbol{\omega}^r_{(t)}\right\rangle_{Y_f} e^{-\lambda^r_{(t)}t}\int_0^t e^{\lambda^r_{(s)}s}\left\langle\boldsymbol{\omega}^r_{(s)}\right\rangle_{Y_f}\cdot\boldsymbol{p}^{dyn}(s,x)\,\mathrm{d}s\ . \qquad (17)$$

Hence, a nonlinear expression of the permeability, the convolution kernel $\boldsymbol{\mathcal{K}}(t,s)$ is obtained, since $(\boldsymbol{\omega}^r_{(t)},\lambda^r_{(t)})$ depend on the micro-deformation of channels Y_f. Below we give more details.

4.1 Dynamic permeability and spectral decomposition

Although $\mathcal{K}$ can be computed using (12), we shall use a different approach which is more convenient to introduce the deformation-dependent permeability later on. For this, we consider the spectral decomposition of the seepage $\boldsymbol{w}$ using the eigenfunctions $\{\boldsymbol{\omega}^r\}_r$ and eigenvalues $\{\lambda^r\}_r$ of the eigenvalue problem: Find $(\boldsymbol{\omega}^r, \pi^r) \in \mathbf{H}^1_{\#0}(Y_f) \times H^1_{\#}(Y_f)$, such that

$$a_f\left(\boldsymbol{\omega}^r,\, \boldsymbol{\psi}\right) + \left\langle \nabla_y \pi^r,\, \boldsymbol{\psi}\right\rangle_{Y_f} = \lambda^r \rho_f \left\langle \boldsymbol{\omega}^r,\, \boldsymbol{\psi}\right\rangle_{Y_f} \ , \quad \left\langle \nabla_y q,\, \boldsymbol{\omega}^r\right\rangle_{Y_f} = 0 \ , \quad \left\langle \boldsymbol{\omega}^r,\, \boldsymbol{\omega}^r\right\rangle_{Y_f} = 1 \ , \tag{18}$$

for all $(\boldsymbol{\psi}, q) \in \mathbf{H}^1_{\#0}(Y_f) \times H^1_{\#}(Y_f)$. Then (10) holds when

$$\hat{\boldsymbol{w}}(t, y, \cdot) = \sum_r \alpha^r(t) \boldsymbol{\omega}^r(y) \ , \quad p^1(t, y, \cdot) = \sum_r \alpha^r(t) \pi^r(y) \ , \tag{19}$$

where $\alpha^r(t)$ is computed upon substituting in (10) and using the orthonormality $\left\langle \boldsymbol{\omega}^s,\, \boldsymbol{\omega}^r\right\rangle_{Y_f} = \delta_{rs}$,

$$\partial_t \alpha^r(t) + \lambda^r \alpha^r(t) = -\boldsymbol{p}^{dyn}(t) \cdot \left\langle \boldsymbol{\omega}^r\right\rangle_{Y_f} \ , \quad \alpha^r(0) = \alpha^r_0 \ , \tag{20}$$

where both $\boldsymbol{p}^{dyn}(t, x)$ and $\alpha^r(t, x)$ depend also on $x \in \Omega$. Using the projection $p^{dyn}_r := \left\langle \boldsymbol{\omega}^r\right\rangle_{Y_f} \cdot \boldsymbol{p}^{dyn}$, we obtain This yields the solution,

$$\begin{aligned} \alpha^r(t) &= e^{-\lambda^r t}\left(\alpha^r_0 + \int_0^t e^{\lambda^r s} \cdot (-p^{dyn}_r)\,\mathrm{d}s\right) \\ &= e^{-\lambda^r t}\left(\alpha^r_0 - \frac{1}{\lambda^r}(e^{\lambda^r t} p^{dyn}_r(t) - p^{dyn}_r(0)) + \int_0^t \frac{e^{\lambda^r s}}{\lambda^r} \frac{\mathrm{d}}{\mathrm{d}\, s} p^{dyn}_r(s)\,\mathrm{d}s\right) \\ &= -p^{dyn}_r(t)/\lambda^r + e^{-\lambda^r t} + \int_0^t \frac{e^{\lambda^r s}}{\lambda^r} \frac{\mathrm{d}}{\mathrm{d}\, s} p^{dyn}_r(s)\,\mathrm{d}s \ , \end{aligned} \tag{21}$$

where we consider $\alpha^r_0 = p^{dyn}_r(0, x)/\lambda^r$. For simplicity we shall assume $p^{dyn}_r(0, x) = 0$ as the initial state.

The dynamic Darcy law The eigenvalue problem (18) can be soved in a perturbed configuration due the microdeformation. Then the eigenpairs $(\boldsymbol{\omega}^r_{(t)}, \lambda^r_{(t)})$ depend on t, which will be indicated by the subscript $_{(t)}$. For this case, (20) must be adapted, so that using the first line in (21) and (19) yield

$$\boldsymbol{w}(t, x) = -\int_0^t \widehat{\mathcal{K}}(t, s) \boldsymbol{p}^{dyn}(s, x)\,\mathrm{d}s = -\sum_r \left\langle \boldsymbol{\omega}^r_{(t)}\right\rangle_{Y_f} e^{-\lambda^r_{(t)} t} \int_0^t e^{\lambda^r_{(s)} s} \left\langle \boldsymbol{\omega}^r_{(s)}\right\rangle_{Y_f} \cdot \boldsymbol{p}^{dyn}(s, x)\,\mathrm{d}s \ . \tag{22}$$

As announced above, a "nonlinear" Darcy law is obtained because of the nonlinear expression of the permeability, the convolution kernel $\mathcal{K}(t, s)$, since the pairs $(\boldsymbol{\omega}^r_{(t)}, \lambda^r_{(t)})$ depend on the micro-deformation of channels Y_f. In this case, we get

$$\begin{aligned} \boldsymbol{w}(t, x) &= -\int_0^t \widehat{\mathcal{K}}(t, s) \boldsymbol{p}^{dyn}(s, x)\,\mathrm{d}s \ , \\ \widehat{\mathcal{K}}(t, s) &= \sum_r \left\langle \boldsymbol{\omega}^r_{(t)}\right\rangle_{Y_f} e^{-\lambda^r_{(t)} t} \otimes e^{\lambda^r_{(s)} s} \left\langle \boldsymbol{\omega}^r_{(s)}\right\rangle_{Y_f} = \bar{\boldsymbol{K}}^r_{(t,s)} e^{-\lambda^r_{(t)} t} e^{\lambda^r_{(s)} s} \ . \end{aligned} \tag{23}$$

where

$$\bar{\boldsymbol{K}}^r_{(t,s)} = \left\langle \boldsymbol{\omega}^r_{(t)} \right\rangle_{Y_f} \otimes \left\langle \boldsymbol{\omega}^r_{(s)} \right\rangle_{Y_f} . \tag{24}$$

For the linear model, thus without the influence of the deformation, $\boldsymbol{\omega}^r$ being independent of the deformation, $\bar{\boldsymbol{K}}^r$ is symmetric. Recall, that $\boldsymbol{\mathcal{K}}(t,s)$ is not symmetric, in general, as the results of the eigenvalues and eigenfuctions associated with different times and, thus, computed for different perturbed configurations, as explained below. A similar effect is observed in the linear case of the acoustic problem under the steady perfusion [11].

Alternatively, the dynamic permeability can be introduced using the third line expression in (21) substituted in (19), such that the convolution involves the time derivative of $\boldsymbol{p}^{dyn}$,

$$\begin{aligned}
\boldsymbol{w}(t,x) &= -\int_0^t \boldsymbol{\mathcal{K}}(t,s) \frac{\mathrm{d}}{\mathrm{d}\, s} \boldsymbol{p}^{dyn}(s,x)\, \mathrm{d}s \\
&= -\sum_r \frac{1}{\lambda^r_{(t)}} \bar{\boldsymbol{K}}^r_{(t,t)} \boldsymbol{p}^{dyn}(t,x) + \sum_r \left\langle \boldsymbol{\omega}^r_{(t)} \right\rangle_{Y_f} e^{-\lambda^r_{(t)} t} \int_0^t \frac{e^{\lambda^r_{(s)} s}}{\lambda_{(s)}} \left\langle \boldsymbol{\omega}^r_{(s)} \right\rangle_{Y_f} \cdot \frac{\mathrm{d}}{\mathrm{d}\, s} \boldsymbol{p}^{dyn}(s,x)\, \mathrm{d}s \\
&= -\sum_r \left(\frac{1}{\lambda^r_{(t)}} \bar{\boldsymbol{K}}^r_{(t,t)} \boldsymbol{p}^{dyn}(t,x) - \int_0^t \widetilde{\boldsymbol{\mathcal{K}}}_{(t,s)}(t,s) \cdot \frac{\mathrm{d}}{\mathrm{d}\, s} \boldsymbol{p}^{dyn}(s,x)\, \mathrm{d}s \right) ,
\end{aligned} \tag{25}$$

where

$$\widetilde{\boldsymbol{\mathcal{K}}}_{(t,s)}(t,s) = \bar{\boldsymbol{K}}^r_{(t,s)} \frac{e^{-\lambda^r_{(t)} t} e^{\lambda^r_{(s)} s}}{\lambda_{(s)}} . \tag{26}$$

This definition of $\widetilde{\boldsymbol{\mathcal{K}}}_{(t,s)}(t,s)$ conforms with the one of the static permeability.

It is worth noting that for the linear (*i.e.* standard) case when (18) is not perturbed), we get in (25)

$$\boldsymbol{\mathcal{K}}(t,s) = -\sum_r \frac{1}{\lambda^r} \bar{\boldsymbol{K}}^r \left(1 - e^{-\lambda^r (t-s)}\right) = \bar{\boldsymbol{\mathcal{K}}} + \widetilde{\boldsymbol{\mathcal{K}}}(t,s) . \tag{27}$$

By virtue of the approach announced in (16), the linearization of the deformation-dependednt permeability defined in (24) and (26) requires the sensitivity analysis of the eigenvalue problem. We can express the total variations of the eigenpairs due to advection velocity field $\vec{\mathcal{V}}$ which transforms the local microconfigurations in terms of perturbed coordinates $z_i(\tau, y) = y_i + \tau \mathcal{V}_i$. Denoting by δ_τ the (partial) directional derivative w.r.t. τ involved in the perturbation, the eignevalue and the averaged eigenvectors can be expressed in terms of the macroscopic responses at time t, as follows

$$\begin{aligned}
\lambda^r_{(t)} &:= \lambda^r_0 + \delta^{\mathrm{tot}}_{(t)} \lambda^r_0 , \\
\left\langle \boldsymbol{\omega}^r_{(t)} \right\rangle_{Y_f} &:= \left\langle \boldsymbol{\omega}^r_0 \right\rangle_{Y_f} + \delta^{\mathrm{tot}}_{(t)} \left\langle \boldsymbol{\omega}^r_0 \right\rangle_{Y_f} ,
\end{aligned} \tag{28}$$

where $\delta^{\mathrm{tot}}_{(t)}()$ presents the total sensitivity w.r.t. the perturbed microconfiguration $z_i(\tau, \cdot)$ with $\vec{\mathcal{V}}$ expressed using the macroscopic responses at time t, see [10].

4.2 The recursive decomposition of the time convolution

For the sake of simplicity, we now consider the linear case, when (27) holds. Then the following recurrent approximation related to the time discretization with time step Δt can be applied to treat the convolution efficiently:

$$
\begin{aligned}
&\bar{\boldsymbol{w}}(t) = -\bar{\boldsymbol{\mathcal{K}}}\boldsymbol{p}^{dyn}(t)\ ,\\
&\tilde{\boldsymbol{w}}(t) = -\int_0^t \widetilde{\boldsymbol{\mathcal{K}}}(t,s)\frac{\mathrm{d}}{\mathrm{d}\,s}\boldsymbol{p}^{dyn}(s)\,\mathrm{d}s = -\left(\int_0^{t-\Delta t}\circ + \int_{t-\Delta t}^{t}\circ\right)\widetilde{\boldsymbol{\mathcal{K}}}(t,s)\frac{\mathrm{d}}{\mathrm{d}\,s}\boldsymbol{p}^{dyn}(s)\,\mathrm{d}s =\\
&\quad = -\sum_r \frac{1}{\lambda^r}\bar{\boldsymbol{K}}^r e^{-\lambda^r\Delta t/2}\left(\boldsymbol{p}^{dyn}(t)-\boldsymbol{p}^{dyn}(t-\Delta t)\right)\\
&\qquad -\sum_r \frac{e^{-\lambda^r\Delta t}}{\lambda^r}\bar{\boldsymbol{K}}^r\int_0^{t-\Delta t} e^{-\lambda^r(t-\Delta t-s)}\frac{\mathrm{d}}{\mathrm{d}\,s}\boldsymbol{p}^{dyn}(s)\,\mathrm{d}s\\
&\quad = -\widetilde{\boldsymbol{\mathcal{K}}}(t,t-\Delta t/2)\left(\boldsymbol{p}^{dyn}(t)-\boldsymbol{p}^{dyn}(t-\Delta t)\right) - \sum_r e^{-\lambda^r\Delta t}\boldsymbol{h}^r(t-\Delta t)\ ,
\end{aligned}
\tag{29}
$$

whereby the recurence yields

$$
\begin{aligned}
&\boldsymbol{h}^r(t) = \frac{e^{-\lambda^r\Delta t/2}}{\lambda^r}\bar{\boldsymbol{K}}^r\left(\boldsymbol{p}^{dyn}(t)-\boldsymbol{p}^{dyn}(t-\Delta t)\right) + \sum_r e^{-\lambda^r\Delta t}\boldsymbol{h}^r(t-\Delta t)\ ,\\
&\text{hence}\quad \boldsymbol{w}(t) = \bar{\boldsymbol{w}}(t)+\tilde{\boldsymbol{w}}(t) = \bar{\boldsymbol{w}}(t) - \sum_r \boldsymbol{h}^r(t)\ .
\end{aligned}
\tag{30}
$$

The extension for the "nonlinear case" is obvious

5 NUMERICAL SIMULATIONS

The two-scale simulation was implemented in the Python based finite element solver *SfePy* [2]. The microscopic subproblems are solved on a representative periodic cell, see Fig. 2, and the homogenized coefficients and their sensitivities with respect to the displacement, pressure, and electric fields are evaluated. For the known coefficients, the nonlinear time-dependent macroscopic problem is solved in an iterative loop. The macroscopic domain Ω with the applied boundary conditions is depicted in Fig. 3.

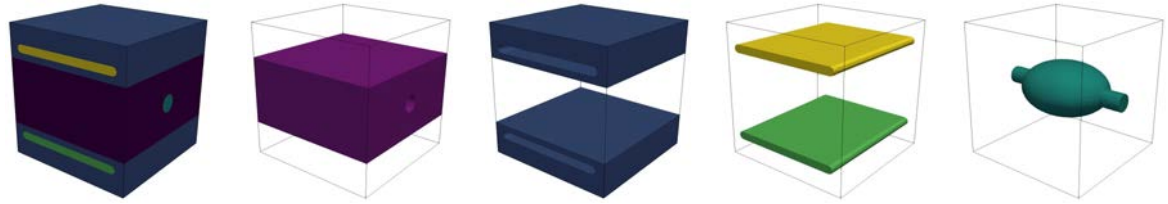

periodic unit cell | elastic part | piezo material | electrodes | fluid

Figure 2: Periodic unit cell and its decomposition.

To illustrate the peristaltic pumping effect in the context of the model nonlinearity, we the cumulative fluxes through the middle face Γ_M obtained in the simulations are compared in Fig. 4 for the linear and non-linear cases, *i.e.* without and with updating the homogenized coefficients using the approximation (16). Positive flux values mean the flow from Γ_L to Γ_R. While in linear case the flux oscillates around zero indicating no effective flux, in the non-linear case, the

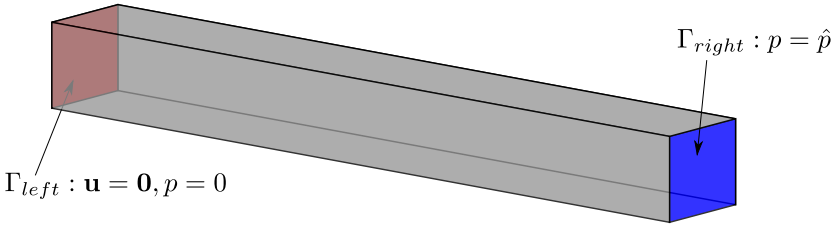

Figure 3: Macroscopic domain Ω with applied boundary conditions.

pumping effect is obvious since the cumulative flux values increase with time, so that the fluid is transported from Γ_L to Γ_R.

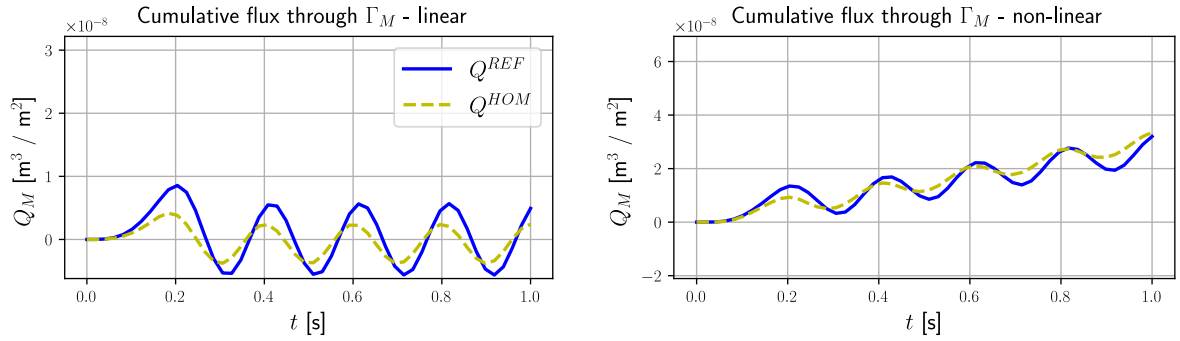

Figure 4: Cumulative flux through the internal faces Γ_M: linear model – left, non-linear model – right.

Further we compare the quasistatic and dynamic responses for the linear models. For the considered low frequency of the electric potential control wave, there is almost no difference. The inertia effect becomes more pronounced with increasing densities ρ_s and ρ_f. In Fig. 5, the differences in the pressure and displacement distribution along the 1D continuum are remarkable for 100 times larger densities.

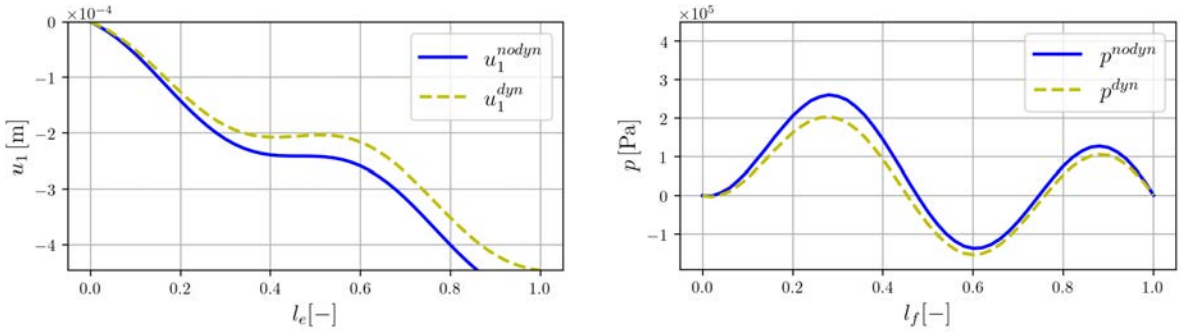

Figure 5: The comparison of the quasistatic and dynamic responses of the displacements and the pressure at a given time instant.

6 CONCLUSIONS

A model of electroactive porous material has been derived using the homogenization of the linearized fluid-structure interaction problem. As confirmed by numerical studies, to achieve the desired pumping effect of the homogenized continuum, it is necessary to account for the

nonlinearity associated with deformation-dependent microconfigurations and, hence, respecting deformation-dependent effective properties of the homogenized material. For this, the sensitivity analysis approach has been applied which leads to a computationally efficient numerical scheme for solving the nonlinear problem. As a new contribution, dynamic aspects of the peristaltic deformation driven flow has been studied in the context of the homogenization. The flow dynamics is reflected by the dynamic Darcy law introducing the time convolution in macroscopic model. A special treatment of the dynamic permeability approximation in terms of the spectral decomposition and its sensitivity analysis required by virtue of the employed approach [9].

The two-scale piezoelectric model respecting the geometrical nonlinearity seems to be an effective tool for simulating peristaltic flows in porous piezoelectric structures. The influence of the flow dynamics and respecting of all the inertia related phenomena is important for higher frequencies of the voltage actuation through the piezoelectric actuators. Further studies and model refinement are envisaged towards using the acoustic wave energy for the fluid transport, in analogy with the "acoustic streaming" phenomenon.

Acknowledgement This research is supported by project GACR 21-16406S of the Czech Scientific Foundation.

REFERENCES

[1] Carew, E.O., Pedley, T.J., An Active Membrane Model for Peristaltic Pumping: Part I-Periodic Activation Waves in an Infinite Tube. Journal of Biomechanical Engineering **119**, 66–76, 1997

[2] Cimrman, R., Lukeš, V., Rohan, E., Multiscale finite element calculations in Python using Sfepy, *Advances in Computational Mathematics*, **45**, 1897–1921, 2019.

[3] Cioranescu, D., Damlamian, A., Griso, G. (2008), The periodic unfolding method in homogenization. *Siam J. Math. Anal.*, **40**(4):1585–1620.

[4] Fung, Y.C., Yih, C.S., Peristaltic Transport. Journal of Applied Mechanics, **35**, 669–675, 1968.

[5] Maiti, S., Misra, J.C., Peristaltic flow of a fluid in a porous channel: A study having relevance to flow of bile within ducts in a pathological state. International Journal of Engineering Science, **49**, 950–966, 2011.

[6] Mikelic, A., 1991. Homogenization of nonstationary Navier-Stokes equations in a domain with a grained boundary. Annali di Matematica Pura ed Applicata 158, 167–179.

[7] Peszyńska, M., Trykozko, A., Forchheimer law in computational and experimental studies of flow through porous media at porescale and mesoscale. In: *Current Advances in Nonlinear Analysis and Related Topics.* **32** of GAKUTO International Series, 463–482, 2010.

[8] Pozrikidis, C., A study of peristaltic flow, Journal of Fluid Mechanics **180**, 515-527, 1987.

[9] Rohan, E., Lukeš, V., Modeling nonlinear phenomena in deforming fluid-saturated porous media using homogenization and sensitivity analysis concepts. *Applied Mathematics and Computation*, **267**, 583–595, 2015.

[10] Rohan, E., Lukeš, V., Homogenization of the fluid-saturated piezoelectric porous media. *International Journal of Solids and Structures*, **147**, 110–125, 2018.

[11] Rohan, E. Naili, S., Homogenization of the fluid-structure interaction in acoustics of porous media perfused by viscous fluid. *Z. Angew. Math. Phys.*, **71**, 137, 2020.

[12] Rohan, E., Lukeš, V., Multiscale modelling of flow due to the peristaltic wave in deforming poro-piezoelectric medium. In: *Proc of the IX Int. Conf. on Computational Meth. for Coupled Problems in Sci. and Engrg., COUPLED PROBLEMS*, 2021, DOI: 10.23967/coupled.2021.037